Leveraging chorionic villus biopsies for the derivation of patient-specific trophoblast stem cells

Kaela M. Varberg[1,†,‡], Ayelen Moreno-Irusta[1,†], Allynson Novoa[2], Brynne Musser[1], Joseph M. Varberg[3], Jeremy P. Goering[4], Irfan Saadi[4], Khursheed Iqbal[1,§], Hiroaki Okae[5], Takahiro Arima[6], John Williams III[7,8], Margareta D. Pisarska[2,7,8,9*], and Michael J. Soares[1,4,10,*]

[1]Institute for Reproductive and Developmental Sciences, Department of Pathology & Laboratory Medicine, University of Kansas Medical Center, Kansas City, KS 66160
[2]Division of Reproductive Endocrinology and Infertility, Department of Obstetrics and Gynecology, Cedars-Sinai Medical Center, Los Angeles, CA
[3]Stowers Institute for Medical Research, Kansas City, MO, 64110
[4]Department of Cell Biology and Physiology, University of Kansas Medical Center, Kansas City, KS 66160
[5]Department of Trophoblast Research, Institute of Molecular Embryology and Genetics, Kumamoto University, Kumamoto 860-0811, Japan
[6]Department of Informative Genetics, Environment and Genome Research Center, Tohoku University Graduate School of Medicine, Sendai 980-8575, Japan
[7]Department of Obstetrics and Gynecology, Cedars-Sinai Medical Center, Los Angeles, CA
[8]David Geffen School of Medicine, University of California, Los Angeles, CA
[9]Department of Biomedical Sciences, Cedars-Sinai Medical Center, Los Angeles, CA
[10]Department of Obstetrics and Gynecology, University of Kansas Medical Center, Kansas City, KS 66160

Running title: Chorionic villus-derived human TS cells

[†]These authors contributed equally.

[‡]Present address: Department of Pediatrics, Children's Mercy Research Institute, Children's Mercy, Kansas City, MO 64108

[§]Present address: Department of Animal and Food Sciences, Oklahoma State University, Stillwater, OK 74078

The authors have declared that no conflict of interest exists.

***Correspondence:**
Margareta D. Pisarska, 8635 West Third Street, Suite 160W, Los Angeles, CA 90048, (310)-423-5763, margareta.pisarska@cshs.org;
Michael J. Soares, Institute for Reproductive and Developmental Sciences, University of Kansas Medical Center, Kansas City, KS, 66160, (913)-588-5691, msoares@kumc.edu

Keywords: trophoblast stem cells, chorionic villus, placental development

Abstract

Human trophoblast stem (**TS**) cells are an informative in vitro model for the generation and testing of biologically meaningful hypotheses. The goal of this project was to derive patient-specific TS cell lines from clinically available chorionic villus sampling biopsies. Cell outgrowths were captured from human chorionic villus tissue specimens cultured in modified human TS cell medium. Cell colonies emerged early during the culture and cell lines were established and passaged for several generations. Karyotypes of the newly established chorionic villus-derived trophoblast stem (**TS^{CV}**) cell lines were determined and compared to initial genetic diagnoses from freshly isolated chorionic villi. Phenotypes of TS^{CV} cells in the stem state and following differentiation were compared to cytotrophoblast-derived TS (**TS^{CT}**) cells. TS^{CV} and TS^{CT} cells uniformly exhibited similarities in the stem state and following differentiation into syncytiotrophoblast and extravillous trophoblast cells. Chorionic villus tissue specimens provide a valuable source for TS cell derivation. They expand the genetic diversity of available TS cells and are associated with defined clinical outcomes. TS^{CV} cell lines provide a new set of experimental tools for investigating trophoblast cell lineage development.

Summary statement

The chorionic villus-derived trophoblast stem cell lines described in this report enhance the genetic diversity of available trophoblast stem cell models and are linked to specific clinical outcomes. They offer a novel set of experimental tools for studying trophoblast cell lineage development and human placentation.

Introduction

The placenta is a critical organ that allows the fetus to develop within the female reproductive tract (Amoroso, 1968). Specialized functions attributed to the placenta are executed by trophoblast cells (Knöfler et al., 2019, Soares et al., 2018, Turco and Moffett,

71 2019). The trophoblast cell lineage arises from the initial differentiation event of the embryo
72 (Rossant and Tam, 2017). In the human, trophoblast cells organize into villous and extravillous
73 structures. A villous is comprised of trophoblast and non-trophoblast cell types and includes a
74 self-renewing trophoblast cell population referred to as cytotrophoblast (Aplin and Jones, 2021,
75 Sun et al., 2020). Cytotrophoblast are the progenitors for two differentiated cell populations:
76 syncytiotrophoblast (**STB**) and extravillous trophoblast cells (**EVT**) (Knöfler et al., 2019, Soares
77 et al., 2018, Turco and Moffett, 2019). STB have a fundamental role in regulating nutrient and
78 waste transfer between mother and fetus (Aplin and Jones, 2021), whereas EVT cells exit the
79 placenta and transform the uterus into an environment supporting placental and fetal
80 development (Knöfler et al., 2019, Soares et al., 2018). Failures in placentation are the root
81 cause of an assortment of disorders of pregnancy, including pregnancy loss, preeclampsia,
82 intrauterine growth restriction, and pre-term birth (Brosens et al., 2019, Burton et al., 2016).
83 Regulatory mechanisms underlying human cytotrophoblast self-renewal and differentiation have
84 largely remained elusive.
85
86 Recently, conditions for capturing and maintaining human trophoblast stem (**TS**) cells in
87 vitro were described (Okae et al., 2018). Human TS cells have the capacity for self-renewal and
88 differentiation into STB cells or EVT. This in vitro model system has led to the generation of new
89 insights into mechanisms regulating human trophoblast cell development (Bhattacharya et al.,
90 2020, Hornbachner et al., 2021, Ishiuchi et al., 2019, Jaju Bhattad et al., 2020, Muto et al.,
91 2021, Perez-Garcia et al., 2021, Ruane et al., 2022, Saha et al., 2020, Shannon et al., 2022,
92 Sheridan et al., 2021, Takahashi et al., 2019, Varberg et al., 2021). Initial human TS cell lines
93 were derived from blastocysts, or first trimester placental tissue obtained from pregnancy
94 terminations. Establishment of culture conditions for human TS cells led to the derivation of TS
95 cells from pluripotent stem cells (Castel et al., 2020, Cinkornpumin et al., 2020, Dong et al.,
96 2020, Guo et al., 2021, Io et al., 2021, Liu et al., 2020, Wei et al., 2021, Yanagida et al., 2021).

97 These in vitro model systems have provided new insights regarding trophoblast cell
98 development; however, it is unknown whether the origin of these TS cells was compatible with a
99 healthy pregnancy outcome.
100
101 Chorionic villus sampling (**CVS**) represents a standard, prenatal care procedure that is
102 performed between 10-14 weeks of gestation (Stranc et al., 1997). Sampling involves the
103 removal of a small amount of chorionic villus tissue, for the purpose of genetic testing. Common
104 indications for retrieving chorionic villus tissue include advanced maternal age, history of
105 infertility, family history (e.g., sibling with genetic anomalies), or an abnormal noninvasive
106 prenatal test result (Pisarska et al., 2016, Stranc et al., 1997). In addition to their use in genetic
107 diagnosis, first trimester chorionic villus tissue has become a robust platform for investigation of
108 placental pathobiology (Flowers et al., 2021, Gonzalez et al., 2021, Pisarska et al., 2016).
109
110 In this study, we derived patient-specific human TS cell lines from clinically available
111 chorionic villus tissue. Derivation of TS cell lines from chorionic villus tissue expands the genetic
112 diversity of available human TS cells and importantly is linked to clinical data describing
113 pregnancy outcomes.

Results

Derivation of TS cells from chorionic villus biopsies

Chorionic villus biopsies were acquired with patient consent as part of standard medical care. Surplus tissue fragments not used for clinical genetic testing were placed in culture medium used for the expansion of human TS cells (Takahashi et al., 2019); **Fig. 1A**). Tissue pieces attached to type IV collagen-coated tissue culture treated plates (**Fig. 1B**). Cell outgrowths were evident at sites of attachment and expanded over the first several weeks of culture (**Fig. 1C**). Cells and tissue fragments were passaged prior to reaching confluency and replated in 24 well plates. Cell colonies emerged after first passage and steadily expanded with culture medium changes every two days. Colony morphology and growth rates were heterogeneous for the first few passages but became more homogenous after 5-6 passages. The morphology of chorionic villus-derived TS (**TS^{CV}**) cells was consistent with the morphology of cytotrophoblast-derived TS cells (**TS^{CT}**; **Fig. 1B, Fig. 2A**). TS^{CV} cell line expansion was carried out slowly to reduce clonal pressure on derived cells. Cell lines were slowly transitioned into 6 well and 10 cm plate formats after passages 3-4 and 7-8, respectively (**Fig. 1C**). Newly established cell lines were cryopreserved beginning at passage 6. Importantly, TS^{CV} cells tolerated cryopreservation. Revived cells survived, attached, and proliferated for further expansion. Overall, TS^{CV} cell line derivation required approximately three months from sample acquisition to functional assessments of derived lines.

The success rate of TS^{CV} line derivation was 42%, with ten TS^{CV} lines (6 XY; 4 XX) successfully derived from 24 unique patient tissue specimens (15 XY; 9 XX; **Table S1**). Success in cell line derivation may be impacted by the negative consequences of overnight shipping or the cellular contents of the tissue fragments but did not appear to be associated with the clinical karyotype of the CVS specimens. Maternal age range was 30-46 with a mean age of 37.3 years. Maternal and paternal ancestries were self-reported and varied (**Table S1**). Chorionic

villus specimen collection ranged from 10-14 weeks gestation with an average gestation age of 12 weeks, 3 days (87 days). The earliest sample was collected at 10 weeks, 6 days gestation and the latest sample was collected at 14 weeks of gestation. The amount of starting tissue available for cell line derivation ranged from 5-20 mg with a mean of 8.5 mg of tissue. Clinical genetics performed on tissue specimens at the time of CVS indicated that 19 samples had normal karyotypes (13 samples 46, XY and 6 samples 46, XX). Clinical karyotyping of the remaining five samples reported genomic abnormalities including two samples with trisomy 18 (47, XX, +18 and 47, XY, +18), one sample with trisomy 21 (47, XX, +21), and two samples with chromosomal translocations (**Table S1**). The ten derived TS^{CV} cell lines were from eight samples with clinically normal karyotypes (TS^{CVK01}, TS^{CVK05}, TS^{CVK09}, TS^{CVK19}, TS^{CVK21}, TS^{CVK22}, TS^{CVK23}, and TS^{CVK24}), one with trisomy 21 (TS^{CVK08}) and one with a translocation (TS^{CVK07}). Additional phenotypic characterization was performed on a subset of TS^{CV} cell lines with 46, XX or 46, XY karyotypes.

Characterization of TS^{CV} cells in the stem state

Karyotyping was repeated on TS^{CV} cells following line derivation and expansion. Cell line karyotypes were largely consistent with the clinical karyotyping (**Table S1**). Karyotypes of TS^{CVK01} and TS^{CVK24} lines were normal and consistent with the clinical results. TS^{CVK09} and TS^{CVK23} cell lines exhibited mosaicism and were not consistent with the clinical results. A subset of the cells karyotyped for TS^{CVK09} were 46, XY. The remaining cells analyzed displayed other genetic anomalies; however, each individual anomaly was restricted to 1-2 total cells (**Table S1**). A subset of TS^{CVK23} cells were identified as mosaic for trisomy 20 (47, XX, +20) following cell line derivation.

TS^{CT27} (XX) and TS^{CT29} (XY) served as reference standard human TS cell lines (Okae et al., 2018) used for comparative characterization of the TS^{CV} cell lines. TS^{CV} cells were

165 maintained in a stem/proliferative state and propagated beyond the Hayflick limit of 50 cell
166 divisions for non-stem cells, which is consistent with TS^{CT} cell proliferation (Okae et al., 2018).
167 Established TS^{CV} cell lines were assessed for presence of mycoplasma by quantitative
168 polymerase chain reaction (**qPCR**) and no evidence of contamination was detected. TS^{CV} cells
169 in the stem state grew in discrete colonies and displayed a cobblestone morphology, consistent
170 with the morphology of cytotrophoblast-derived cell lines, TS^{CT27} and TS^{CT29} ((Okae et al., 2018);
171 **Fig. 2A**). TS^{CV} cells displayed additional characteristics consistent with their trophoblast cell
172 identity (Lee et al., 2016), including expression of microRNAs from the Chromosome 19
173 microRNA cluster (**Fig. 2B; C19MC**; hsa-miR-517a-3p, has-miR-517-5p, and hsa-miR-526b-3p)
174 and hypomethylation of the E74 Like ETS Transcription Factor 5 (***ELF5)*** promoter relative to
175 induced pluripotent stem (**iPS**) cells (**Fig. 2C**). Overall, TS^{CV} and TS^{CT} cells cultured in the stem
176 state displayed similar proliferative, morphologic, microRNA expression, and methylation
177 properties.
178
179 **Analysis of the differentiation capacity of TS^{CV} cells**
180 Comparisons of TS^{CV} and TS^{CT} cell capacities for differentiation into STB and EVT cell
181 lineages, were performed following cell line derivation (**Fig. 1C**). Assessments of cell
182 differentiation were routinely performed following 10 passages. Differentiation was assessed at
183 morphological and functional levels.
184
185 ***STB differentiation****.* The ability of TS^{CV} cells to differentiate into STB was assessed
186 using the previously described three-dimensional STB (**ST3D**) protocol (Okae et al., 2018). STB
187 differentiation elicited significant morphological changes, including the formation of suspended
188 spheroid cell clusters (**Fig. 3A**). Complementary to the morphological changes observed, TS^{CV}-
189 derived STB displayed downregulation of stem state transcripts ***TEAD4***, ***LRP2***, and ***LIN28A***
190 (**Fig. 3B**) and upregulation of STB lineage-specific transcripts, including cytochrome P450

191 Family 11 Subfamily 1 (***CYP11A1***), chorionic gonadotropin beta 7 (***CGB7***), and syndecan 1
192 (***SDC1***; **Fig. 3C**). STB differentiated from TS^{CV} cells secreted chorionic gonadotropin (**CG**) at
193 levels comparable to STB differentiated from TS^{CT} cells as measured by ELISA (**Fig. 3D**).
194 Overall, TS^{CV}-derived STB had similar cell morphology, expression patterns of signature STB
195 transcripts, and CG production that is observed in TS^{CT}-derived STB.
196
197 ***EVT cell differentiation.*** Canonical features of EVT cell differentiation observed in TS^{CT}
198 cells were evident in TS^{CV} cell lines with normal karyotypes (TS^{CVK01}, TS^{CVK09}, TS^{CVK23}, and
199 TS^{CVK24}), including elongated cell morphology (**Fig. 4A; Videos 1-3**) and expression of major
200 histocompatibility complex, class I, G (**HLA-G**) protein (**Fig. 4B**). EVT cells displayed
201 downregulation of stem state transcripts ***TEAD4***, ***LRP2***, and ***LIN28A*** (**Fig. 4C**). Characteristic
202 EVT transcripts were upregulated, including *HLA-G*, matrix metallopeptidase 2 (***MMP2***), and C-
203 C motif chemokine receptor 1 (***CCR1***; **Fig. 4D**). Overall, these TS^{CV} stem cell derived EVT cells
204 were comparable to EVT cells derived from TS^{CT} cells.
205
206 **Transcriptomic analysis of the developmental potential of TS^{CV} cells**
207 To obtain a broad comparative assessment of TS^{CV} and TS^{CT} in stem, STB, and EVT
208 differentiated cell states, transcriptomes were captured using RNA-sequencing (**RNA-seq**). STB
209 differentiation from the stem state resulted in broad changes in gene expression in TS^{CT} cells
210 (TS^{CT27}, TS^{CT29}; **Fig. 5A; Table S2**) and TS^{CV} cells (TS^{CVK01}, TS^{CVK09}, TS^{CVK23}, and TS^{CVK24}; **Fig.**
211 **5B; Table S3**), including downregulation of stem markers *EPCAM, LIN28A, LRP2, PEG10,* and
212 *TEAD4* and upregulation of STB markers *CGB2, CGB7, CYP11A1*, *CYP19A1,* and *SDC1*. STB
213 differentiation-induced changes in gene expression were consistent between TS^{CT} (TS^{CT27} and
214 TS^{CT29}) and TS^{CV} (TS^{CVK01}, TS^{CVK09}, TS^{CVK23}, and TS^{CVK24}) cells (R=0.87, p<2.23-16; **Fig. 5C**).
215 EVT cells successfully differentiated from the stem state exhibited broad gene
216 expression changes in TS^{CT} (TS^{CT27}, TS^{CT29}; **Fig. 5D; Table S4**) and TS^{CV} cell lines with normal

217 karyotypes (TS^{CVK01}, TS^{CVK09}, TS^{CVK23}, and TS^{CVK24}; **Fig. 5E; Table S5**). These changes included
218 the downregulation of stem markers *EPCAM, LIN28A, LRP2, PEG10,* and *TEAD4* and
219 upregulation of EVT cell markers *CCR1, HLA-G, ITGA1*, *MMP2,* and *NOTUM*. Gene expression
220 changes induced by EVT cell differentiation were consistent between TS^{CT} (TS^{CT27} and TS^{CT29})
221 and TS^{CV} (TS^{CVK01}, TS^{CVK09}, TS^{CVK23}, and TS^{CVK24}) cells (R=0.85, p<2.23-16; **Fig. 5F**).
222 Principal component analysis of TS^{CT} and TS^{CV} cell lines identified three primary cell-
223 state specific clusters (**Fig. 5G**). TS^{CV} cells displayed consistent clustering in the stem state and
224 following STB and EVT cell lineage differentiation (**Fig. 5G**). Results from correlation analyses
225 performed to compare cell expression profiles are indicative of comparable transcriptomic
226 changes across TS^{CV} and TS^{CT} cell lines (**Fig. 5H**). Overall, these results indicate that TS^{CV} cells
227 are capable of self-renewal and effective differentiation into both STB and EVT cell lineages and
228 can be considered bonafide TS cells.
229
230 **Discussion**
231 Our understanding of placenta development and function has benefitted from the
232 availability of in vitro model systems. In the human, these model systems have included primary
233 cell and explant cultures, choriocarcinoma-derived cell lines, and immortalized cell lines (Ringler
234 and Strauss, 1990, Shibata et al., 2020). Each in vitro approach has had merits but also
235 limitations (Lee et al., 2016, Soares et al., 2018). Over two decades ago, Rossant and
236 colleagues reported a procedure for culturing TS cells from the mouse (Tanaka et al., 1998).
237 These cells could be maintained in a proliferative stem state or induced to differentiate.
238 Furthermore TS cells could be reintroduced into blastocysts and shown to possess the capacity
239 to contribute to mouse placentas (Tanaka et al., 1998). Mouse TS cells became an effective
240 model system to elucidate gene regulatory networks controlling trophoblast cell differentiation
241 and placental development (Hada et al., 2022, Hemberger et al., 2020, Latos and Hemberger,
242 2016, Lee et al., 2019). Efforts ensued to establish TS cells in other species with some success

243 (Asanoma et al., 2011, Grigor'eva et al., 2009) but human TS cells represented an enigma
244 (Kunath et al., 2014, Shibata et al., 2020). Culture protocols for sustaining mouse TS cells were
245 ineffective in the human (Kunath et al., 2014). The discovery of culture conditions for
246 propagating and differentiating human TS cells represented a major advancement (Okae et al.,
247 2018). Utilizing these human TS cell culture tools, we have demonstrated the feasibility of
248 capturing and expanding authentic TS cells from human chorionic villus specimens. Unique to
249 these newly derived stem cells is the ability to obtain clinical outcomes that can be used to study
250 placental development leading to healthy outcomes and disease states.
251
252 The initial human TS cell lines were derived from either blastocysts or first trimester
253 pregnancy terminations (Okae et al., 2018). These human TS cell lines represent the
254 benchmark for all TS cell lines subsequently derived. Chorionic villus biopsies are an alternative
255 tissue source for deriving TS cells. They are retrieved during the first trimester of pregnancy as
256 part of standard medical care (Adusumalli et al., 2007, Dong et al., 2003, McIntosh et al., 1993,
257 Pisarska et al., 2016, Stranc et al., 1997, Wang et al., 1994, Williams et al., 1992, Williams et
258 al., 1987). Thus, chorionic villus-derived TS cell lines can be connected to robust pregnancy
259 outcome information. Human TS cell lines have also been derived from miscarriages (Saha et
260 al., 2020), term human placenta tissue (Wang et al., 2022), and reprogrammed from pluripotent
261 stem cells (Castel et al., 2020, Cinkornpumin et al., 2020, Dong et al., 2020, Guo et al., 2021, Io
262 et al., 2021, Jang et al., 2022, Liu et al., 2020, Soncin et al., 2022, Viukov et al., 2022, Wei et
263 al., 2021, Yanagida et al., 2021). These alternative TS cell models are potentially useful tools for
264 investigating trophoblast cell development but each offer caveats for consideration. TS cells
265 derived from trophoblast tissue obtained from miscarriages may best contribute to
266 understanding trophoblast cell-related mechanisms linked to pregnancy failure and the impact of
267 a failed pregnancy on TS cells. TS cells recovered from term placental tissue reflect the
268 culmination of events transpiring throughout the duration of pregnancy, as epigenomic

269 differences are observed in the placenta during gestation (Flowers et al., 2021, Gonzalez et al.,
270 2021). Pluripotency is established through extensive genomic reprogramming (Hanna et al.,
271 2010, Papp and Plath, 2013), which minimizes the impact of the epigenetic landscape
272 established during pregnancy on the TS cell phenotype. It is reasonable to assume that genetic
273 background and source of trophoblast tissue for TS derivation will influence TS cell behavior.
274 Culturing TS cells under optimized conditions may normalize some features attributed to an
275 adverse pregnancy and maternal environment, whereas in other cases the aberrant behavior
276 may persist. Advantages of using chorionic villus-derived TS cells for investigating trophoblast
277 cell-gene regulatory networks contributing to placental development are evident.
278
279 TS cell lines were successfully derived from chorionic villus biopsies possessing both
280 normal and abnormal karyotypes. TS cells with a triploid karyotype have also been established
281 from human blastocysts (Kong et al., 2022). Most recently, trophoblast organoids with abnormal
282 karyotypes have been derived from chorionic villus biopsies (Schaffers et al., 2022). Chorionic
283 villus-derived TS cell lines could be interrogated in the stem state and following differentiation
284 into either STB or EVT cell lineages. The phenotypic and functional parameters evaluated
285 revealed similarities between cytotrophoblast and chorionic villus-derived TS cells when
286 cultured for stem state maintenance or following STB and EVT cell differentiation. Some
287 differences in the capacity for EVT cell differentiation among chorionic villus-derived TS cells
288 were noted. Variability in the capacity for human TS cell line differentiation into EVT cells has
289 been previously reported (Cinkornpumin et al., 2020, Haider et al., 2022, Okae et al., 2018,
290 Shannon et al., 2022). Numerous factors such as unreported clinical characteristics, undetected
291 genomic differences, or inherent sample variability could be contributing to the differences
292 observed. Thus, chorionic villus-derived TS cells represent a unique in vitro model to investigate
293 functional variability in TS cells isolated from a temporally relevant tissue source. The true
294 impact of the chromosomal abnormalities on TS cells and their differentiation into STB or EVT

295 cells will require successful cultivation and characterization of multiple cell lines possessing the
296 same abnormal karyotype.
297
298 Mosaicism is a characteristic feature of the human placenta (Coorens et al., 2021,
299 Robinson and Del Gobbo, 2021, Yuen and Robinson, 2011). Trophoblast cells possess a
300 tolerance for karyotypic abnormalities not evident in the embryo or fetus (Coorens et al., 2021,
301 Shahbazi et al., 2020, Yuen and Robinson, 2011). Each cotyledon of the placenta exhibits
302 elements of trophoblast cell clonality (Coorens et al., 2021). Placental mosaicism is manifested
303 in genetic and functional differences among cotyledons within a human placenta (Coorens et al.,
304 2021, Huang et al., 2009, Rubin et al., 1993, Wang et al., 1993). Among the TS cell lines
305 derived from chorionic villus biopsies, some exhibited a karyotype consistent with the karyotype
306 of chorionic villus tissue used for the clinical genetic analysis, whereas others differed. Chorionic
307 villus biopsies contain a mixture of trophoblast and extraembryonic mesoderm (Aplin and Jones,
308 2021). Thus, differences in TS cell versus chorionic villus tissue could be attributed to confined
309 placental mosaicism or alternatively, linked to an unappreciated consequence of culture
310 conditions required to establish the TS cell lines.
311
312 In summary, the generation of chorionic villus biopsy-derived human TS cell lines
313 expand the genetic diversity of existing TS cell lines available for basic research and importantly
314 provides an opportunity to associate pregnancy outcomes with trophoblast cell biology. The
315 research also offers insights into the significance of genetic anomalies and mosaicism in
316 trophoblast cell development and introduces a novel precision medicine approach to the study
317 of placentation.
318
319 **Materials and Methods**
320 **Chorionic villus tissue collections, karyotypic analysis, and clinical phenotyping**

321 Chorionic villus tissue was obtained by highly experienced perinatologists as part of
322 standard medical care between 10-14 weeks of gestation for clinical genetic diagnosis at
323 Cedars-Sinai Medical Center (Huang et al., 2009, Pisarska et al., 2016). Clinical cytogenetic
324 analysis was performed on tissue specimens by direct and long-term culture and reviewed by a
325 team of cytogeneticists (Huang et al., 2009). Residual trophoblast tissue fragments not required
326 for clinical cytogenetic analysis were recovered, suspended in Complete TS Cell Medium
327 [DMEM/F12 (11320033, Thermo Fisher, Waltham, MA), 100 μM 2-mercaptoethanol, 0.2%
328 (vol/vol) fetal bovine serum (**FBS**), 50 μM penicillin, 50 U/mL streptomycin, 0.3% bovine serum
329 albumin (**BSA**, BP9704100, Thermo Fisher), 1% Insulin-Transferrin-Selenium-Ethanolamine
330 (**ITS-X**) solution (vol/vol, 51500056, Thermo Fisher)], 8.5 μM L-ascorbic acid (A8960, Sigma-
331 Aldrich, St. Louis, MO), 50 ng/mL epidermal growth factor (**EGF**, E9644, Sigma-Aldrich), 2 μM
332 CHIR99021 (04-0004, Reprocell, Beltsville, MD), 0.5 μM A83-01 (04-0014, Reprocell), 1 μM
333 SB431542 (04-0010, Reprocell), 800 μM valproic acid (P4543, Sigma-Aldrich), and 5 μM
334 Y27632 (04-0012-02, Reprocell)] (Okae et al., 2018), shipped overnight to the University of
335 Kansas Medical Center, and used for TS cell derivation. Demographic data was collected from
336 patients and included, parental ages, races and ethnicities, and ancestry (**Table S1**).
337

338 **Derivation of TS cells from chorionic villus tissue specimens**

339 Chorionic villus biopsy tissue fragments were dissected and transferred in complete
340 human TS cell medium. Briefly, individual villus fragments were minced and transferred to a
341 1.7mL tube, washed with PBS, and centrifuged at 500 x g for 3 min. Tissue pellets were
342 resuspended in HBSS (with Ca^{2+} and Mg^{2+}) supplemented with 1.25U/ml dispase II, 0.4mg/ml
343 collagenase IV and 80 U/ml DNase I. Samples were then agitated for 15 min at 37ºC. After
344 incubation, tissue suspensions were centrifuged at 500 x g for 3 min. and washed with basal TS
345 cell medium. Finally, cells and tissue suspensions were centrifuged at 500 x g for 3 min,
346 resuspended in complete human TS cell medium and plated in 5 mg/mL Corning® mouse type

347 IV collagen (35623, Discovery Labware Inc., Billerica, MA) coated dishes containing complete
348 human TS cell medium. Cells and remaining tissue fragments attached within 2-5 days. Medium
349 was replaced with fresh TS cell culture medium after initial attachment and every two days
350 thereafter. Time to first passage was unique to each sample and determined by the extent of the
351 outgrowth, but commonly occurred around 21 days post plating. Cells and attached tissue
352 fragments were washed with PBS and detached with TrypLE Express (12604021, Thermo
353 Fisher). Cell and tissue fragments were replated in human TS cell culture conditions in a 24 well
354 plate format. Colonies emerged after the first passage. Cells were maintained in 24 well plate
355 format for 3-5 passages and then expanded into 6 well plate format.
356
357 **TS cell culture**
358 Following TS cell derivation, TS cells were cultured in dishes pre-coated with iMatrix511
359 (1:2000 dilution; NP892-01, Reprocell). TS cells were maintained in Modified Complete TS Cell
360 Medium [DMEM/F12 (11320033, Thermo Fisher), 50 U/mL penicillin, 50 µg/mL streptomycin,
361 0.15% BSA (BP9704100, Thermo Fisher), 1% ITS-X solution (vol/vol; 51500056, Thermo
362 Fisher)], 200 µM L-ascorbic acid (A8960, Sigma-Aldrich), 1% KnockOut Serum Replacement
363 (**KSR**, 10828028, Thermo Fisher), 25 ng/mL EGF (E9644, Sigma-Aldrich), 2 µM CHIR99021
364 (04-0004, Reprocell), 5 µM A83-01 (04-0014, Reprocell), 800 µM valproic acid (P4543, Sigma-
365 Aldrich), and 2.5 µM Y27632 (04-0012-02, Reprocell)] (Takahashi et al., 2019) medium was
366 replaced every two days of culture. TS^{CT27} (XX) and TS^{CT29} (XY) (Okae et al., 2018) were used
367 as reference lines.
368
369 **STB differentiation**
370 To induce STB cell differentiation, TS cells were plated into 6 cm petri dishes at a
371 density of 300,000 cells per dish and cultured in ST3D Medium [DMEM/F12 (11320033, Thermo
372 Fisher), 50 U/mL penicillin, 50 µg/mL streptomycin, 0.15% BSA (BP9704100, Thermo Fisher),

373 1% ITS-X solution (vol/vol; 51500056, Thermo-Fisher)], 200 μM L-ascorbic acid (A8960, Sigma-
374 Aldrich), 5% KSR (10828028, Thermo Fisher), 2.5 μM Y27632 (04-0012, Reprocell), 2 μM
375 forskolin (F6886, Sigma-Aldrich), and 50 ng/mL of EGF (E9644, Sigma-Aldrich)](Okae et al.,
376 2018). On day 3 of cell differentiation, 3 mL of fresh ST3D medium was added to the culture
377 dishes. Cells were analyzed on day 6 of STB cell differentiation.
378
379 **EVT cell differentiation**
380 EVT cell differentiation was induced by plating human TS cells onto 6-well plates pre-
381 coated with 1 μg/mL of mouse type IV collagen at a density of 80,000 cells per well. Cells were
382 cultured in EVT Differentiation Medium [DMEM/F12 (11320033, Thermo Fisher), 100 μm 2-
383 mercaptoethanol, 50 U/mL penicillin, 50 μg/mL streptomycin, 0.3% bovine serum albumin
384 (BP9704100, Thermo Fisher), 1% Insulin-Transferrin-Selenium-Ethanolamine solution (vol/vol;
385 51500056, Thermo Fisher)], 100 ng/mL of neuregulin 1 (**NRG1**, 5218SC, Cell Signaling,
386 Danvers, MA), 7.5 μM A83-01 (04-0014, Reprocell), 2.5 μM Y27632 (04-0012, Reprocell), 4%
387 KSR (10828028, Thermo Fisher), and 2% Matrigel® (CB-40234, Thermo Fisher). On day 3 of
388 EVT cell differentiation, the medium was replaced with EVT Differentiation Medium excluding
389 NRG1 and with a reduced Matrigel® concentration of 0.5%. On day 6 of EVT cell differentiation,
390 the medium was replaced with EVT Differentiation Medium with a Matrigel® concentration of
391 0.5% and excluding NRG1 and KSR. Cells were analyzed on day 8 of EVT cell differentiation.
392
393 **Cell line karyotyping**
394 Chromosome analysis of TS^{CV} cells was performed using standard cytogenetic methods
395 (Huang et al., 2009, Pisarska et al., 2016). GTG banded chromosomes were analyzed at 450-
396 550 band levels. Cytogenetic and fluorescence in situ hybridization results were described
397 according to the current International Standing Committee on Human Cytogenetic
398 Nomenclature (ISCN, 2009).

399

400 **Immunocytochemical analysis**

401 Cells were fixed with 4% paraformaldehyde (Sigma-Aldrich) for 15 min at room
402 temperature. Fixed cells were incubated with primary antibody against HLA-G (ab52455,
403 Abcam), followed by Alexa488-conjugated goat-anti-mouse immunoglobulin G (**IgG**; A32723,
404 Thermo Fisher Scientific) secondary antibody and 4′,6-diamidino-2-phenylindole (**DAPI**;
405 Molecular Probes, Eugene, OR). Fluorescence images were captured on a Nikon 80i upright
406 microscope (Nikon) with a Photometrics CoolSNAP-ES monochrome camera (Roper
407 Technologies, Inc., Sarasota, FL).

408

409 **iPS cell culture**

410 Human iPS cells were propagated in tissue culture plates pre-coated with Matrigel®
411 (1:100 dilution; 356231, Corning Life Sciences, Tewksbury, MA). iPS cells were maintained in
412 complete iPS Cell Medium [mTeSR1 Basal Medium + mTeSR1 5X Supplement (85850,
413 STEMCELL Technologies, Inc., Vancouver, CA) and 10 μM Y27632 (04-0012-02, Reprocell)]
414 and incubated at 37°C and 5% CO_2. After the first day of culture, cells were cultured in complete
415 iPS cell medium without Y27632. Medium was replaced every other day of culture. Cells were
416 passaged or harvested at 80% confluency.

417

418 **miRNA isolation, cDNA preparation, and quantitative real-time PCR**

419 Total RNA was isolated using mirVana kit (AM1560, Thermo Fisher), and RNA
420 concentration was measured with the Qubit™ RNA BR Assay Kit (Thermo Fisher). cDNA
421 synthesis was performed with TaqMan® Advanced miRNA cDNA Synthesis kit (A28007,
422 Thermo Fisher). RT-qPCR was performed using TaqMan™Fast Advanced Master Mix
423 (4444556, Thermo Fisher) and targeted miRNAs MIR517a-3p, MIR517-5p, MIR-526b-3p, and
424 housekeeping miRNA MIR103a-3p (479485_mir, 478996_mir, and 478253_mir; TaqMan™

425 Advanced miRNA Assays, Thermo Fisher; **Table S6**). Relative expression of each transcript
426 was calculated using ΔΔCT method and normalized to hsa-miR-103a-3p.
427
428 **Methylation analysis**
429 Genomic DNA was isolated using the DNeasy Blood and Tissue Kit (69504, Qiagen,
430 Germantown, MD), and 500 ng of DNA was bisulfite converted using the EZ DNA Methylation-
431 Gold Kit (D5005, Zymo Research, Irvine, CA) according to instructions. Following bisulfite
432 conversion, the ELF5 promoter region was amplified using a nested PCR approach with
433 previously reported primers (Primer Set A: forward: 5'-GGAAATGATGGATATTGAATTTGA-3';
434 reverse: 5'-CAATAAAAATAAAAACACCTATAACC-3' Primer Set B: forward: 5'-
435 GAGGTTTTAATATTGGGTTTATAATG-3'; reverse: 5'-ATAAATAACACCTACAAACAAATCC-3';
436 **Table S7**; (Lee et al., 2016, Soncin et al., 2022). PCR was performed with a hot start DNA
437 polymerase, ZymoTaq (E2001, Zymo Research). After the second PCR, Taq polymerase-
438 amplified PCR products were gel-purified with QIAquick Gel Extraction Kit (28706X4, Qiagen),
439 using manufacturer protocols. The purified DNA was inserted directly into a plasmid vector
440 using TOPO® TA Cloning® Kits for Sequencing (450030, Thermo Fisher) according to
441 manufacturer instructions. One microliter of purified PCR product was cloned into the plasmid
442 vector (pCR™4-TOPO®) for 5 min at room temperature. Competent *E. coli* cells were
443 transformed with the pCR4-TOPO construct, cultured, and minipreps were prepared using the
444 QIAprep Spin Miniprep Kit (27106X4, Qiagen). Purified DNA was sequenced (GENEWIZ, South
445 Plainfield, NJ).
446
447 **CG enzyme-linked immunosorbent assay (ELISA)**
448 Conditioned medium was collected following six days of STB culture for each cell line.
449 CG levels were measured using an ELISA kit (HC251F, Calbiotech), following the
450 manufacturer's protocol. The measurements were normalized to total cell protein content.

451

452 **RNA isolation and RT-qPCR**

453 Total RNA was isolated using TRIzol®/chloroform precipitation (15596018, Thermo
454 Fisher) as previously reported (Varberg et al., 2021). cDNA was synthesized from 1 μg of total
455 RNA using the High-Capacity cDNA Reverse Transcription Kit (4368813, Thermo Fisher) and
456 diluted 10 times with ultra-pure distilled water. qPCR was performed using PowerSYBR® Green
457 PCR Master Mix (4367659, Thermo Fisher) and primers (250 nM each). RT-qPCR primer
458 sequences are presented in **Table S8**. Amplification and fluorescence detection were measured
459 with a QuantStudio 5 Flex Real-Time PCR System (Thermo Fisher). An initial step (95°C, 10
460 min) preceded 40 cycles of a two-step PCR (92°C, 15 s; 60°C, 1 min) and was followed by a
461 dissociation step (95°C, 15 s; 60°C, 15 s; 95°C 15 s). The comparative cycle threshold method
462 was used for relative quantification of the amount of mRNA for each sample normalized to the
463 housekeeping genes *B2M* or *POLR2A*.

464

465 **RNA library preparation and RNA-Seq**

466 Stranded mRNA-sequencing was performed on the Illumina NovaSeq 6000 Sequencing
467 System in the Genomics Core at the University of Kansas Medical Center. Quality control was
468 completed with the RNA Screen Tape Assay kit (5067-5576, Agilent Technologies, Santa Clara,
469 CA) on the Agilent TapeStation 4200. Total RNA (1 µg) was processed in the following steps: i)
470 oligo dT bead capture of mRNA, ii) fragmentation, iii) reverse transcription, iv) cDNA end repair,
471 v) Unique Dual Index (**UDI**) adaptor ligation, vi) strand selection, and vii) library amplification
472 using the Universal Plus mRNA-Seq with NuQuant library preparation kit (0520-A01, Tecan
473 Genomics, Männedorf, Switzerland). Library validation was performed with the D1000 Screen
474 Tape Assay kit (5067-5582, Agilent Technologies) on the Agilent Tape Station 4200. Library
475 concentrations were determined with the NuQuant module using a Qubit 4 Fluorometer (Thermo

476 Fisher). Libraries were pooled based on equal molar amounts and the multiplexed pool was
477 quantified, in triplicate, using the Roche Lightcycler96 with FastStart Essential DNA Green
478 Master (06402712001, Roche, Indianapolis, IN) and KAPA Library Quant (Illumina, Inc., San
479 Diego, CA) DNA Standards 1-6 (KK4903, KAPA Biosystems, Wilmington, MA). Using the qPCR
480 results, the RNA-Seq library pool was adjusted to 2.125 nM for multiplexed sequencing. Pooled
481 libraries were denatured with 0.2 N NaOH (0.04N final concentration), neutralized with 400 mM
482 Tris-HCl, pH 8.0, and diluted to 425 pM. Onboard clonal clustering of the patterned flow cell was
483 performed using the NovaSeq 6000 S1 Reagent Kit (200 cycle, 20012864, Illumina). A 2x101
484 cycle sequencing profile with dual index reads was completed using the following sequence
485 profile: Read 1 – 101 cycles x Index Read 1 – 8 cycles x Index Read 2 – 8 cycles x Read 2 –
486 101 cycles. Sequence data were converted from .bcl to FASTQ file format using bcl2fastq
487 software and de-multiplexed. Raw FASTQ files were trimmed using default parameters (-r 0.1 -d
488 0.03) in Skewer (Version 0.2.2) and reads shorter than 18 bp were discarded. Transcripts were
489 quantified using Kallisto (Version 0.46.2). Differentially expressed genes (FDR of 0.05) were
490 discovered using the Bioconductor package DESeq2 in R (Version 1.32.0).
491
492 **Live cell imaging**
493 Cells were placed into an EVOS Onstage Incubator attached to an EVOS FL Automated
494 Imaging System (Thermo Fisher). The live cell chamber was maintained at constant
495 temperature (37ºC), humidity, and 5% CO_2. For stem culture, TS cells were maintained in stem
496 state culture conditions described above and images were acquired 1-2 days after passage and
497 immediately following culture medium change. EVT cell differentiation was induced as described
498 above. On the fourth day of the EVT cell differentiation protocol, cells were placed into the live
499 cell chamber. Phase contrast images were acquired every 10 min continuously from days 2-4 of
500 stem cell growth or day 4-6 of EVT cell differentiation.
501

502 **Mycoplasma testing**

503 Mycoplasma presence was assessed using the LookOut® Mycoplasma qPCR Detection
504 Kit (MP0040A, Sigma-Aldrich). Kit protocols were followed as described.

505

506 **Data availability**

507 All raw and processed sequencing data generated in this study have been submitted to
508 the NCBI Gene Expression Omnibus (GEO; https://www.ncbi.nlm.nih.gov/geo/).

509

510 **Code availability**

511 Only publicly available tools were used for data analysis and are described where
512 relevant in the methods.

513

514 **Materials availability**

515 Materials will be made available upon reasonable request to the investigators.

516

517 **Statistical analysis**

518 Statistical analysis was completed with the GraphPad Prism 9 software. Welch's *t* tests,
519 Brown-Forsythe and Welch ANOVA tests were applied when appropriate. The figures depict the
520 data represented as mean ± standard deviation with a statistical significance level of $p<0.05$.

521

522 **Study Approval**

523 All human tissue specimens used for research purposes were collected following
524 informed written consent, deidentified, and approved by institutional review boards at both
525 Cedars-Sinai Medical Center and at the University of Kansas Medical Center.

526

527 **Acknowledgements**

We thank Stacy Oxley and Brandi Miller for their administrative assistance and Clark Bloomer and Rosanne Skinner in the KUMC Genome Sequencing Facility for their work in library preparation and DNA sequencing. The research was supported by a National Institutes of Health (**NIH**) National Research Service Award postdoctoral fellowship (F32HD096809) and pathway to independence award (K99HD107262) to K.M.V., NIH grants (MDP: AI154535; MJS: HD020676, HD099638, HD105734), and the Sosland Foundation.

Author contributions

K.M.V., A.M., M.D.P, and M.J.S. conceived and designed the research; A.N., J.W., and M.D.P. collected and obtained tissue specimens. J.G., I.S., H.O., and T.A. provided reagents, protocols, or equipment; K.M.V., A.M., B.M., and K.I., performed experiments and/or analyzed data; K.M.V, A.M., J.G, I.S., M.D.P, and M.J.S. interpreted results of experiments; K.M.V., A.M., J.M.V., and M.J.S. prepared figures and drafted manuscript; K.M.V., A.M., M.D.P, and M.J.S. edited and revised manuscript; All authors approved final version of manuscript.

Competing Interest Statement

There is no conflict of interest that could be perceived as prejudicing the impartiality of the research reported.

Diversity and inclusion statement

We are committed to promote diversity and inclusion in our research. Our team comprises individuals from varied backgrounds, and we seek to ensure equitable representation and recognition in our work and collaborations.

550 **References**

551

552 ADUSUMALLI, J., HAN, C. S., BECKHAM, S., BARTHOLOMEW, M. L. & WILLIAMS, J.
553 2007. Chorionic villus sampling and risk for hypertensive disorders of pregnancy.
554 *American Journal of Obstetrics and Gynecology,* 196**,** 591.e1-7; discussion 591.e7.
555 AMOROSO, E. C. 1968. The evolution of viviparity. *Proceedings of the Royal Society of*
556 *Medicine,* 61**,** 1188-1200.
557 APLIN, J. D. & JONES, C. J. P. 2021. Cell dynamics in human villous trophoblast. *Human*
558 *Reproduction Update,* 27**,** 904-922.
559 ASANOMA, K., RUMI, M. A. K., KENT, L. N., CHAKRABORTY, D., RENAUD, S. J.,
560 WAKE, N., LEE, D.-S., KUBOTA, K. & SOARES, M. J. 2011. FGF4-dependent stem
561 cells derived from rat blastocysts differentiate along the trophoblast lineage.
562 *Developmental Biology,* 351**,** 110-119.
563 BHATTACHARYA, B., HOME, P., GANGULY, A., RAY, S., GHOSH, A., ISLAM, M. R.,
564 FRENCH, V., MARSH, C., GUNEWARDENA, S., OKAE, H., ARIMA, T. & PAUL, S.
565 2020. Atypical protein kinase C iota (PKCλ/ι) ensures mammalian development by
566 establishing the maternal-fetal exchange interface. *Proceedings of the National Academy*
567 *of Sciences of the United States of America,* 117**,** 14280-14291.
568 BROSENS, I., PUTTEMANS, P. & BENAGIANO, G. 2019. Placental bed research: I. The
569 placental bed: from spiral arteries remodeling to the great obstetrical syndromes.
570 *American Journal of Obstetrics and Gynecology,* 221**,** 437-456.
571 BURTON, G. J., FOWDEN, A. L. & THORNBURG, K. L. 2016. Placental origins of chronic
572 disease. *Physiological Reviews,* 96**,** 1509-1565.
573 CASTEL, G., MEISTERMANN, D., BRETIN, B., FIRMIN, J., BLIN, J., LOUBERSAC, S.,
574 BRUNEAU, A., CHEVOLLEAU, S., KILENS, S., CHARIAU, C., GAIGNERIE, A.,
575 FRANCHETEAU, Q., KAGAWA, H., CHARPENTIER, E., FLIPPE, L., FRANÇOIS-
576 CAMPION, V., HAIDER, S., DIETRICH, B., KNÖFLER, M., ARIMA, T., BOURDON,
577 J., RIVRON, N., MASSON, D., FOURNIER, T., OKAE, H., FRÉOUR, T. & DAVID, L.
578 2020. Induction of human trophoblast stem cells from somatic cells and pluripotent stem
579 cells. *Cell Reports,* 33**,** 108419.
580 CINKORNPUMIN, J. K., KWON, S. Y., GUO, Y., HOSSAIN, I., SIROIS, J., RUSSETT, C. S.,
581 TSENG, H.-W., OKAE, H., ARIMA, T., DUCHAINE, T. F., LIU, W. & PASTOR, W.
582 A. 2020. Naive human embryonic stem cells can give rise to cells with a trophoblast-like
583 transcriptome and methylome. *Stem Cell Reports,* 15**,** 198-213.
584 COORENS, T. H. H., OLIVER, T. R. W., SANGHVI, R., SOVIO, U., COOK, E., VENTO-
585 TORMO, R., HANIFFA, M., YOUNG, M. D., RAHBARI, R., SEBIRE, N.,
586 CAMPBELL, P. J., CHARNOCK-JONES, D. S., SMITH, G. C. S. & BEHJATI, S. 2021.
587 Inherent mosaicism and extensive mutation of human placentas. *Nature,* 592**,** 80-85.
588 DONG, C., BELTCHEVA, M., GONTARZ, P., ZHANG, B., POPLI, P., FISCHER, L. A.,
589 KHAN, S. A., PARK, K.-M., YOON, E.-J., XING, X., KOMMAGANI, R., WANG, T.,
590 SOLNICA-KREZEL, L. & THEUNISSEN, T. W. 2020. Derivation of trophoblast stem
591 cells from naïve human pluripotent stem cells. *eLife,* 9**,** e52504.
592 DONG, L., FALK, R. E., WILLIAMS, J., KOHAN, M. & SCHRECK, R. R. 2003. Tetrasomy
593 12p--unusual presentation in CVS. *Prenatal Diagnosis,* 23**,** 101-103.
594 FLOWERS, A. E., GONZALEZ, T. L., JOSHI, N. V., EISMAN, L. E., CLARK, E. L.,
595 BUTTLE, R. A., SAURO, E., DIPENTINO, R., LIN, Y., WU, D., WANG, Y.,

596 SANTISKULVONG, C., TANG, J., LEE, B., SUN, T., CHAN, J. L., WANG, E. T.,
597 JEFFERIES, C., LAWRENSON, K., ZHU, Y., AFSHAR, Y., TSENG, H.-R.,
598 WILLIAMS, J. & PISARSKA, M. D. 2021. Sex differences in microRNA expression in
599 first and third trimester human placenta†. *Biology of Reproduction*, ioab221.
600 GONZALEZ, T. L., EISMAN, L. E., JOSHI, N. V., FLOWERS, A. E., WU, D., WANG, Y.,
601 SANTISKULVONG, C., TANG, J., BUTTLE, R. A., SAURO, E., CLARK, E. L.,
602 DIPENTINO, R., JEFFERIES, C. A., CHAN, J. L., LIN, Y., ZHU, Y., AFSHAR, Y.,
603 TSENG, H.-R., TAYLOR, K., WILLIAMS, J. & PISARSKA, M. D. 2021. High-
604 throughput miRNA sequencing of the human placenta: expression throughout gestation.
605 *Epigenomics,* 13, 995-1012.
606 GRIGOR'EVA, E. V., SHEVCHENKO, A. I., MAZUROK, N. A., ELISAPHENKO, E. A.,
607 ZHELEZOVA, A. I., SHILOV, A. G., DYBAN, P. A., DYBAN, A. P., NONIASHVILI,
608 E. M., SLOBODYANYUK, S. Y., NESTEROVA, T. B., BROCKDORFF, N. &
609 ZAKIAN, S. M. 2009. FGF4 Independent Derivation of Trophoblast Stem Cells from the
610 Common Vole. *PLoS ONE,* 4, e7161.
611 GUO, G., STIRPARO, G. G., STRAWBRIDGE, S. E., SPINDLOW, D., YANG, J., CLARKE,
612 J., DATTANI, A., YANAGIDA, A., LI, M. A., MYERS, S., ÖZEL, B. N., NICHOLS, J.
613 & SMITH, A. 2021. Human naive epiblast cells possess unrestricted lineage potential.
614 *Cell Stem Cell,* 28, 1040-1056.e6.
615 HADA, M., MIURA, H., TANIGAWA, A., MATOBA, S., INOUE, K., OGONUKI, N.,
616 HIROSE, M., WATANABE, N., NAKATO, R., FUJIKI, K., HASEGAWA, A.,
617 SAKASHITA, A., OKAE, H., MIURA, K., SHIKATA, D., ARIMA, T., SHIRAHIGE,
618 K., HIRATANI, I. & OGURA, A. 2022. Highly rigid H3.1/H3.2-H3K9me3 domains set
619 a barrier for cell fate reprogramming in trophoblast stem cells. *Genes & Development,* 36,
620 84-102.
621 HAIDER, S., LACKNER, A. I., DIETRICH, B., KUNIHS, V., HASLINGER, P.,
622 MEINHARDT, G., MAXIAN, T., SALEH, L., FIALA, C., POLLHEIMER, J., LATOS,
623 P. A. & KNÖFLER, M. 2022. Transforming growth factor-β signaling governs the
624 differentiation program of extravillous trophoblasts in the developing human placenta.
625 *Proceedings of the National Academy of Sciences of the United States of America,* 119,
626 e2120667119.
627 HANNA, J. H., SAHA, K. & JAENISCH, R. 2010. Pluripotency and cellular reprogramming:
628 facts, hypotheses, unresolved issues. *Cell,* 143, 508-525.
629 HEMBERGER, M., HANNA, C. W. & DEAN, W. 2020. Mechanisms of early placental
630 development in mouse and humans. *Nature Reviews. Genetics,* 21, 27-43.
631 HORNBACHNER, R., LACKNER, A., PAPUCHOVA, H., HAIDER, S., KNÖFLER, M.,
632 MECHTLER, K. & LATOS, P. A. 2021. MSX2 safeguards syncytiotrophoblast fate of
633 human trophoblast stem cells. *Proceedings of the National Academy of Sciences of the*
634 *United States of America,* 118, e2105130118.
635 HUANG, A., ADUSUMALLI, J., PATEL, S., LIEM, J., WILLIAMS, J. & PISARSKA, M. D.
636 2009. Prevalence of chromosomal mosaicism in pregnancies from couples with
637 infertility. *Fertility and Sterility,* 91, 2355-2360.
638 IO, S., KABATA, M., IEMURA, Y., SEMI, K., MORONE, N., MINAGAWA, A., WANG, B.,
639 OKAMOTO, I., NAKAMURA, T., KOJIMA, Y., IWATANI, C., TSUCHIYA, H.,
640 KASWANDY, B., KONDOH, E., KANEKO, S., WOLTJEN, K., SAITOU, M.,
641 YAMAMOTO, T., MANDAI, M. & TAKASHIMA, Y. 2021. Capturing human

642 trophoblast development with naive pluripotent stem cells in vitro. *Cell Stem Cell,* 28**,**
643 1023-1039.e13.
644 ISCN 2009. *ISCN (2009): An international system for human cytogenetic nomenclature,* Basel,
645 Karger S.
646 ISHIUCHI, T., OHISHI, H., SATO, T., KAMIMURA, S., YORINO, M., ABE, S., SUZUKI, A.,
647 WAKAYAMA, T., SUYAMA, M. & SASAKI, H. 2019. Zfp281 shapes the
648 transcriptome of trophoblast stem cells and Is essential for placental development. *Cell*
649 *Reports,* 27**,** 1742-1754.e6.
650 JAJU BHATTAD, G., JEYARAJAH, M. J., MCGILL, M. G., DUMEAUX, V., OKAE, H.,
651 ARIMA, T., LAJOIE, P., BÉRUBÉ, N. G. & RENAUD, S. J. 2020. Histone deacetylase
652 1 and 2 drive differentiation and fusion of progenitor cells in human placental
653 trophoblasts. *Cell Death & Disease,* 11**,** 311.
654 JANG, Y. J., KIM, M., LEE, B.-K. & KIM, J. 2022. Induction of human trophoblast stem-like
655 cells from primed pluripotent stem cells. *Proceedings of the National Academy of*
656 *Sciences of the United States of America,* 119**,** e2115709119.
657 KNÖFLER, M., HAIDER, S., SALEH, L., POLLHEIMER, J., GAMAGE, T. K. J. B. &
658 JAMES, J. 2019. Human placenta and trophoblast development: key molecular
659 mechanisms and model systems. *Cellular and molecular life sciences: CMLS,* 76**,** 3479-
660 3496.
661 KONG, X., CHEN, X., OU, S., WANG, W. & LI, R. 2022. Derivation of human triploid
662 trophoblast stem cells. *Journal of Assisted Reproduction and Genetics,* 39**,** 1183-1193.
663 KUNATH, T., YAMANAKA, Y., DETMAR, J., MACPHEE, D., CANIGGIA, I., ROSSANT, J.
664 & JURISICOVA, A. 2014. Developmental differences in the expression of FGF receptors
665 between human and mouse embryos. *Placenta,* 35**,** 1079-1088.
666 LATOS, P. A. & HEMBERGER, M. 2016. From the stem of the placental tree: trophoblast stem
667 cells and their progeny. *Development (Cambridge, England),* 143**,** 3650-3660.
668 LEE, B.-K., JANG, Y. J., KIM, M., LEBLANC, L., RHEE, C., LEE, J., BECK, S., SHEN, W. &
669 KIM, J. 2019. Super-enhancer-guided mapping of regulatory networks controlling mouse
670 trophoblast stem cells. *Nature Communications,* 10**,** 4749.
671 LEE, C. Q. E., GARDNER, L., TURCO, M., ZHAO, N., MURRAY, M. J., COLEMAN, N.,
672 ROSSANT, J., HEMBERGER, M. & MOFFETT, A. 2016. What is trophoblast? A
673 combination of criteria define human first-trimester trophoblast. *Stem Cell Reports,* 6**,**
674 257-272.
675 LIU, X., OUYANG, J. F., ROSSELLO, F. J., TAN, J. P., DAVIDSON, K. C., VALDES, D. S.,
676 SCHRÖDER, J., SUN, Y. B. Y., CHEN, J., KNAUPP, A. S., SUN, G., CHY, H. S.,
677 HUANG, Z., PFLUEGER, J., FIRAS, J., TANO, V., BUCKBERRY, S., PAYNTER, J.
678 M., LARCOMBE, M. R., POPPE, D., CHOO, X. Y., O'BRIEN, C. M., PASTOR, W. A.,
679 CHEN, D., LEICHTER, A. L., NAEEM, H., TRIPATHI, P., DAS, P. P., GRUBMAN,
680 A., POWELL, D. R., LASLETT, A. L., DAVID, L., NILSSON, S. K., CLARK, A. T.,
681 LISTER, R., NEFZGER, C. M., MARTELOTTO, L. G., RACKHAM, O. J. L. & POLO,
682 J. M. 2020. Reprogramming roadmap reveals route to human induced trophoblast stem
683 cells. *Nature,* 586**,** 101-107.
684 MCINTOSH, N., RUBIN, C., WANG, B. & WILLIAMS, J. 1993. Transcervical CVS sample
685 size: correlation with placental location, cytogenetic findings, and pregnancy outcome.
686 *Prenatal Diagnosis,* 13**,** 1031-1036.

687 MUTO, M., CHAKRABORTY, D., VARBERG, K. M., MORENO-IRUSTA, A., IQBAL, K.,
688 SCOTT, R. L., MCNALLY, R. P., CHOUDHURY, R. H., APLIN, J. D., OKAE, H.,
689 ARIMA, T., MATSUMOTO, S., EMA, M., MAST, A. E., GRUNDBERG, E. &
690 SOARES, M. J. 2021. Intersection of regulatory pathways controlling hemostasis and
691 hemochorial placentation. *Proceedings of the National Academy of Sciences of the United*
692 *States of America,* 118**,** e2111267118.
693 OKAE, H., TOH, H., SATO, T., HIURA, H., TAKAHASHI, S., SHIRANE, K., KABAYAMA,
694 Y., SUYAMA, M., SASAKI, H. & ARIMA, T. 2018. Derivation of human trophoblast
695 stem cells. *Cell Stem Cell,* 22**,** 50-63.e6.
696 PAPP, B. & PLATH, K. 2013. Epigenetics of reprogramming to induced pluripotency. *Cell,* 152**,**
697 1324-1343.
698 PEREZ-GARCIA, V., LEA, G., LOPEZ-JIMENEZ, P., OKKENHAUG, H., BURTON, G. J.,
699 MOFFETT, A., TURCO, M. Y. & HEMBERGER, M. 2021. BAP1/ASXL complex
700 modulation regulates epithelial-mesenchymal transition during trophoblast differentiation
701 and invasion. *eLife,* 10**,** e63254.
702 PISARSKA, M. D., AKHLAGHPOUR, M., LEE, B., BARLOW, G. M., XU, N., WANG, E. T.,
703 MACKEY, A. J., FARBER, C. R., RICH, S. S., ROTTER, J. I., CHEN, Y.-D. I.,
704 GOODARZI, M. O., GULLER, S. & WILLIAMS, J. 2016. Optimization of techniques
705 for multiple platform testing in small, precious samples such as human chorionic villus
706 sampling. *Prenatal Diagnosis,* 36**,** 1061-1070.
707 RINGLER, G. E. & STRAUSS, J. F. 1990. In vitro systems for the study of human placental
708 endocrine function. *Endocrine Reviews,* 11**,** 105-123.
709 ROBINSON, W. P. & DEL GOBBO, G. F. 2021. Mistakes Are Common; Should We Worry
710 about Them? *Trends in Molecular Medicine,* 27**,** 721-722.
711 ROSSANT, J. & TAM, P. P. L. 2017. New Insights into Early Human Development: Lessons for
712 Stem Cell Derivation and Differentiation. *Cell Stem Cell,* 20**,** 18-28.
713 RUANE, P. T., GARNER, T., PARSONS, L., BABBINGTON, P. A., WANGSAPUTRA, I.,
714 KIMBER, S. J., STEVENS, A., WESTWOOD, M., BRISON, D. R. & APLIN, J. D.
715 2022. Trophectoderm differentiation to invasive syncytiotrophoblast is promoted by
716 endometrial epithelial cells during human embryo implantation. *Human Reproduction*
717 *(Oxford, England),* 37**,** 777-792.
718 RUBIN, C. H., WILLIAMS, J. & WANG, B. B. 1993. Discrepancy in mosaic findings between
719 chorionic villi and amniocytes: a diagnostic dilemma involving 45,X, 46,XY, and
720 47,XYY cell lines. *American Journal of Medical Genetics,* 46**,** 457-459.
721 SAHA, B., GANGULY, A., HOME, P., BHATTACHARYA, B., RAY, S., GHOSH, A., RUMI,
722 M. A. K., MARSH, C., FRENCH, V. A., GUNEWARDENA, S. & PAUL, S. 2020.
723 TEAD4 ensures postimplantation development by promoting trophoblast self-renewal:
724 An implication in early human pregnancy loss. *Proceedings of the National Academy of*
725 *Sciences of the United States of America,* 117**,** 17864-17875.
726 SCHAFFERS, O. J. M., DUPONT, C., BINDELS, E. M., VAN OPSTAL, D., DEKKERS, D. H.
727 W., DEMMERS, J. A. A., GRIBNAU, J. & RIJN, B. B. V. 2022. Single-Cell Atlas of
728 Patient-Derived Trophoblast Organoids in Ongoing Pregnancies. *Organoids,* 1**,** 106-115.
729 SHAHBAZI, M. N., WANG, T., TAO, X., WEATHERBEE, B. A. T., SUN, L., ZHAN, Y.,
730 KELLER, L., SMITH, G. D., PELLICER, A., SCOTT, R. T., SELI, E. & ZERNICKA-
731 GOETZ, M. 2020. Developmental potential of aneuploid human embryos cultured
732 beyond implantation. *Nature Communications,* 11**,** 3987.

733 SHANNON, M. J., BALTAYEVA, J., CASTELLANA, B., WÄCHTER, J., MCNEILL, G. L.,
734 YOON, J. S., TREISSMAN, J., LE, H. T., LAVOIE, P. M. & BERISTAIN, A. G. 2022.
735 Cell trajectory modeling identifies a primitive trophoblast state defined by BCAM
736 enrichment. *Development (Cambridge, England),* 149**,** dev199840.
737 SHERIDAN, M. A., ZHAO, X., FERNANDO, R. C., GARDNER, L., PEREZ-GARCIA, V., LI,
738 Q., MARSH, S. G. E., HAMILTON, R., MOFFETT, A. & TURCO, M. Y. 2021.
739 Characterization of primary models of human trophoblast. *Development (Cambridge,*
740 *England),* 148**,** dev199749.
741 SHIBATA, S., KOBAYASHI, E. H., KOBAYASHI, N., OIKE, A., OKAE, H. & ARIMA, T.
742 2020. Unique features and emerging in vitro models of human placental development.
743 *Reproductive Medicine and Biology,* 19**,** 301-313.
744 SOARES, M. J., VARBERG, K. M. & IQBAL, K. 2018. Hemochorial placentation:
745 development, function, and adaptations†. *Biology of Reproduction,* 99**,** 196-211.
746 SONCIN, F., MOREY, R., BUI, T., REQUENA, D. F., CHEUNG, V. C., KALLOL, S.,
747 KITTLE, R., JACKSON, M. G., FARAH, O., DUMDIE, J., MEADS, M., PIZZO, D.,
748 HORII, M., FISCH, K. M. & PARAST, M. M. 2022. Derivation of functional trophoblast
749 stem cells from primed human pluripotent stem cells. *Stem Cell Reports,* 17**,** 1303-1317.
750 STRANC, L. C., EVANS, J. A. & HAMERTON, J. L. 1997. Chorionic villus sampling and
751 amniocentesis for prenatal diagnosis. *Lancet (London, England),* 349**,** 711-714.
752 SUN, T., GONZALEZ, T. L., DENG, N., DIPENTINO, R., CLARK, E. L., LEE, B., TANG, J.,
753 WANG, Y., STRIPP, B. R., YAO, C., TSENG, H.-R., KARUMANCHI, S. A.,
754 KOEPPEL, A. F., TURNER, S. D., FARBER, C. R., RICH, S. S., WANG, E. T.,
755 WILLIAMS, J. & PISARSKA, M. D. 2020. Sexually Dimorphic Crosstalk at the
756 Maternal-Fetal Interface. *The Journal of Clinical Endocrinology and Metabolism,* 105**,**
757 dgaa503.
758 TAKAHASHI, S., OKAE, H., KOBAYASHI, N., KITAMURA, A., KUMADA, K.,
759 YAEGASHI, N. & ARIMA, T. 2019. Loss of p57KIP2 expression confers resistance to
760 contact inhibition in human androgenetic trophoblast stem cells. *Proceedings of the*
761 *National Academy of Sciences of the United States of America*.
762 TANAKA, S., KUNATH, T., HADJANTONAKIS, A. K., NAGY, A. & ROSSANT, J. 1998.
763 Promotion of trophoblast stem cell proliferation by FGF4. *Science (New York, N.Y.),* 282**,**
764 2072-2075.
765 TURCO, M. Y. & MOFFETT, A. 2019. Development of the human placenta. *Development,* 146**,**
766 dev163428.
767 VARBERG, K. M., IQBAL, K., MUTO, M., SIMON, M. E., SCOTT, R. L., KOZAI, K.,
768 CHOUDHURY, R. H., APLIN, J. D., BISWELL, R., GIBSON, M., OKAE, H., ARIMA,
769 T., VIVIAN, J. L., GRUNDBERG, E. & SOARES, M. J. 2021. ASCL2 reciprocally
770 controls key trophoblast lineage decisions during hemochorial placenta development.
771 *Proceedings of the National Academy of Sciences of the United States of America,* 118.
772 VIUKOV, S., SHANI, T., BAYERL, J., AGUILERA-CASTREJON, A., OLDAK, B.,
773 SHEBAN, D., TARAZI, S., STELZER, Y., HANNA, J. H. & NOVERSHTERN, N.
774 2022. Human primed and naïve PSCs are both able to differentiate into trophoblast stem
775 cells. *Stem Cell Reports***,** S2213-6711(22)00457-X.
776 WANG, B. B., RUBIN, C. H. & WILLIAMS, J. 1993. Mosaicism in chorionic villus sampling:
777 an analysis of incidence and chromosomes involved in 2612 consecutive cases. *Prenatal*
778 *Diagnosis,* 13**,** 179-190.

779 WANG, B. T., PENG, W., CHENG, K. T., CHIU, S. F., HO, W., KHAN, Y., WITTMAN, M. &
780 WILLIAMS, J. 1994. Chorionic villi sampling: laboratory experience with 4,000
781 consecutive cases. *American Journal of Medical Genetics,* 53**,** 307-316.
782 WANG, L.-J., CHEN, C.-P., LEE, Y.-S., NG, P.-S., CHANG, G.-D., PAO, Y.-H., LO, H.-F.,
783 PENG, C.-H., CHEONG, M.-L. & CHEN, H. 2022. Functional antagonism between
784 ΔNp63α and GCM1 regulates human trophoblast stemness and differentiation. *Nature*
785 *Communications,* 13**,** 1626.
786 WEI, Y., WANG, T., MA, L., ZHANG, Y., ZHAO, Y., LYE, K., XIAO, L., CHEN, C., WANG,
787 Z., MA, Y., ZHOU, X., SUN, F., LI, W., DUNK, C., LI, S., NAGY, A., YU, Y., PAN,
788 G., LYE, S. J. & SHAN, Y. 2021. Efficient derivation of human trophoblast stem cells
789 from primed pluripotent stem cells. *Science Advances,* 7**,** eabf4416.
790 WILLIAMS, J., MEDEARIS, A. L., CHU, W. H., KOVACS, G. D. & KABACK, M. M. 1987.
791 Maternal cell contamination in cultured chorionic villi: comparison of chromosome Q-
792 polymorphisms derived from villi, fetal skin, and maternal lymphocytes. *Prenatal*
793 *Diagnosis,* 7**,** 315-322.
794 WILLIAMS, J., WANG, B. B., RUBIN, C. H. & AIKEN-HUNTING, D. 1992. Chorionic villus
795 sampling: experience with 3016 cases performed by a single operator. *Obstetrics and*
796 *Gynecology,* 80**,** 1023-1029.
797 YANAGIDA, A., SPINDLOW, D., NICHOLS, J., DATTANI, A., SMITH, A. & GUO, G. 2021.
798 Naive stem cell blastocyst model captures human embryo lineage segregation. *Cell Stem*
799 *Cell,* 28**,** 1016-1022.e4.
800 YUEN, R. K. C. & ROBINSON, W. P. 2011. Review: A high capacity of the human placenta for
801 genetic and epigenetic variation: implications for assessing pregnancy outcome.
802 *Placenta,* 32 Suppl 2**,** S136-141.
803

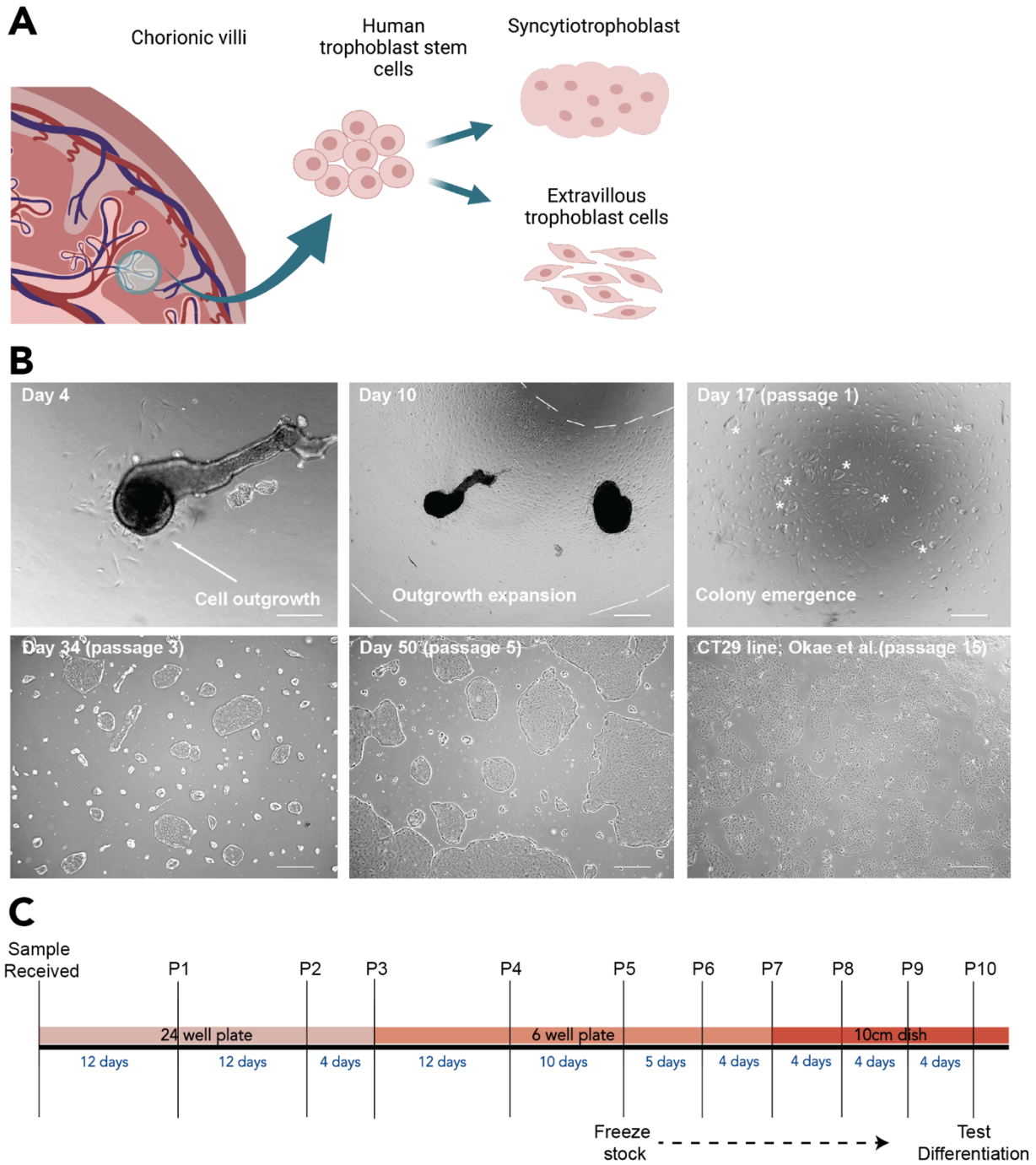

Fig. 1 Deriving TS cells from chorionic villus tissue specimens. A) Simplified schematic depicting the process of obtaining chorionic villi tissue fragments, derivation of TS cells, and then subsequent differentiation into STB and EVT cell lineages. Created with BioRender.com. **B)** Chorionic villus tissue fragments attach and form cellular outgrowths within a few days of initial plating. Within one to two weeks the outgrowths expand and proliferate across the well. Two to three weeks after plating, the cells were passaged, and colonies emerged. Colony clusters were initially small but proliferated and grew rapidly. Significant heterogeneity is present initially, but subsequent passaging selects for a TS cell population that displays a similar morphology to the original TS cell lines (Okae et al., 2018), which possess the ability to

813 differentiate into STB and EVT cell lineages. Scale bar represents 250 μm in first panel. All
814 other scale bars represent 500 μm. **C)** An example timeline for TS cell line derivation and
815 characterization.

816

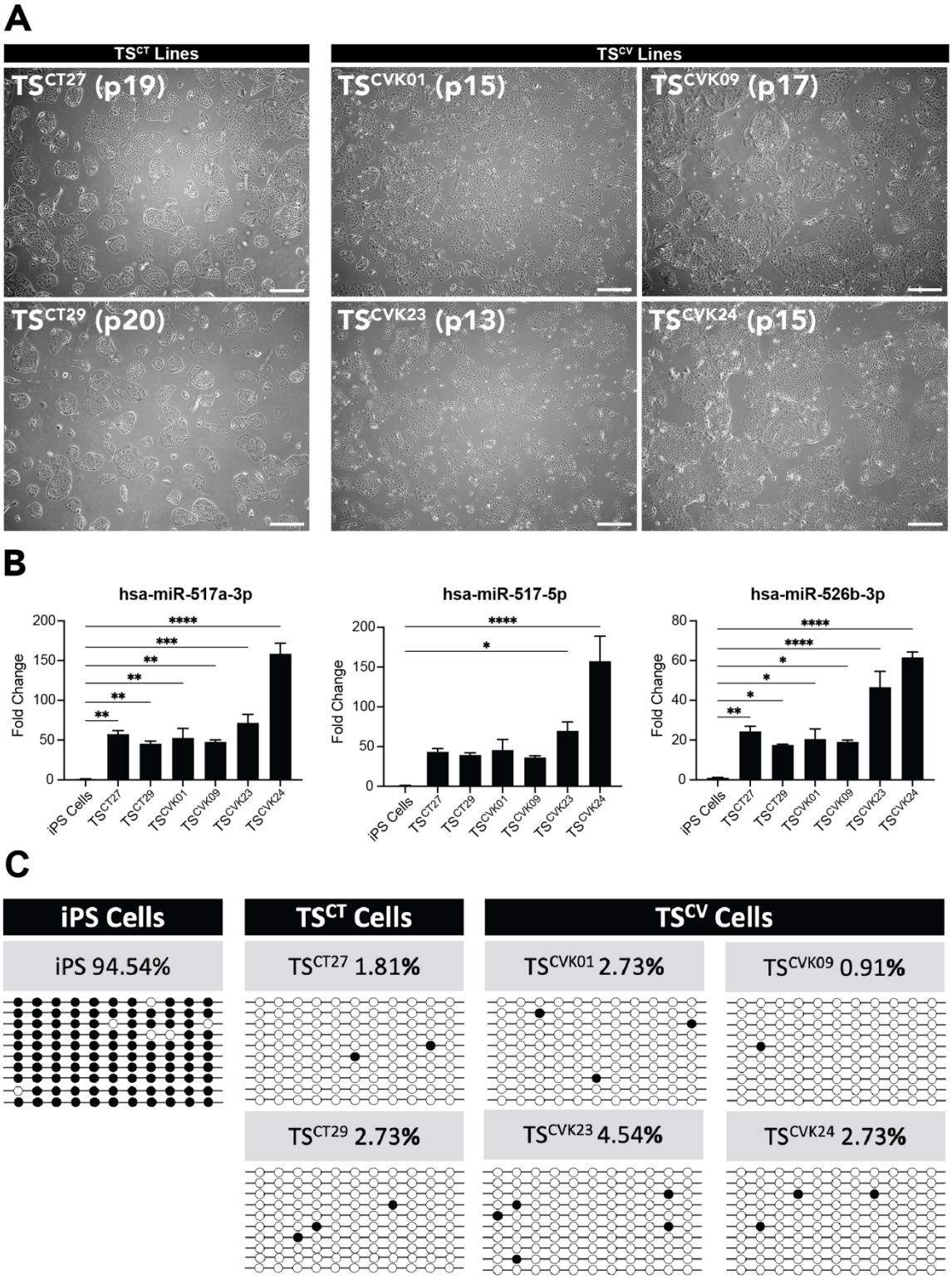

817 **Fig. 2 Characterization of TS^{CV} cells. A)** Stem state phase contrast images of four chorionic
818 villus-derived TS cell lines (TS^{CVK01}, TS^{CVK09}, TS^{CVK23}, TS^{CVK24}) alongside images of the
819 reference cytotrophoblast-derived TS cell lines (TS^{CT27} and TS^{CT29}) at different passage

820 numbers (13-20). Scale bars represent 500 μm. **B)** Bar graphs depicting expression of three
821 microRNAs (**miR**) from the C19MC cluster (hsa-miR-517a-3p, has-miR-517-5p, and hsa-miR-
822 526b-3p) in TS^{CT} and TS^{CV} cell lines relative to induced pluripotent stem (**iPS**) cells, measured
823 by RT-qPCR. Data were normalized to the control miRNA, hsa-miR-103a-3p (n=3 samples per
824 group; *$p<0.05$, **$p<0.01$, ***$p<0.001$, ****$p<0.0001$). **C)** Plots representing DNA methylation
825 levels in the ELF5 promoter at 11 sites in TS^{CT} and TS^{CV} cell lines compared to iPS cells.
826 Methylated sites (black) and unmethylated sites (white) are shown for 10 replicates and the
827 average percent methylation is listed.

Fig. 3

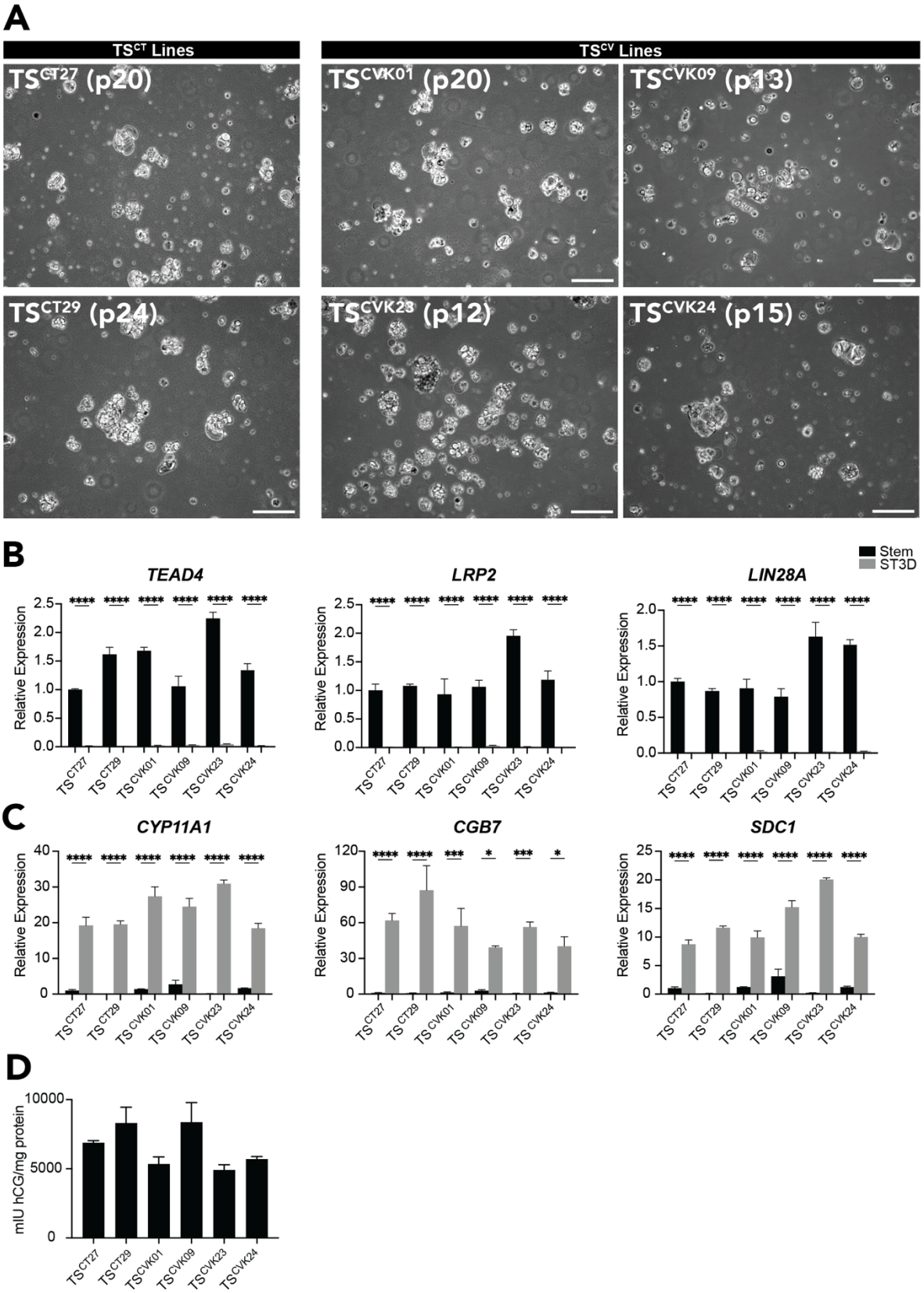

830 **TS^{CV} cell line differentiation into STB. A)** Representative phase contrast images of

831 cytotrophoblast-derived TS^{CT27} and TS^{CT29} cells and four chorionic villus-derived TS cell lines
832 possessing a normal karyotype, TS^{CVK01}, TS^{CVK09}, TS^{CVK23}, and TS^{CVK24} cultured under STB
833 differentiation conditions. Scale bars represent 250 µm. **B-C)** Stem cell-associated transcripts
834 (**B;** *TEAD4*, *LRP2*, and *LIN28A*) and STB cell-associated transcripts (**C**; *CYP11A1, CGB7,* and
835 *SDC1*) were quantified by RT-qPCR in stem (black) and STB differentiated (gray) TS^{CT27},
836 TS^{CT29}, TS^{CVK01}, TS^{CVK09}, TS^{CVK23}, and TS^{CVK24} cells (n=3 samples per group; **p<0.01,
837 ***p<0.001, ****p<0.0001). **D)** Chorionic gonadotropin (**CG**) protein levels (mIU/mg protein) were
838 quantified by ELISA in cell culture supernatants collected from TS^{CT} and TS^{CV} cultured cells.

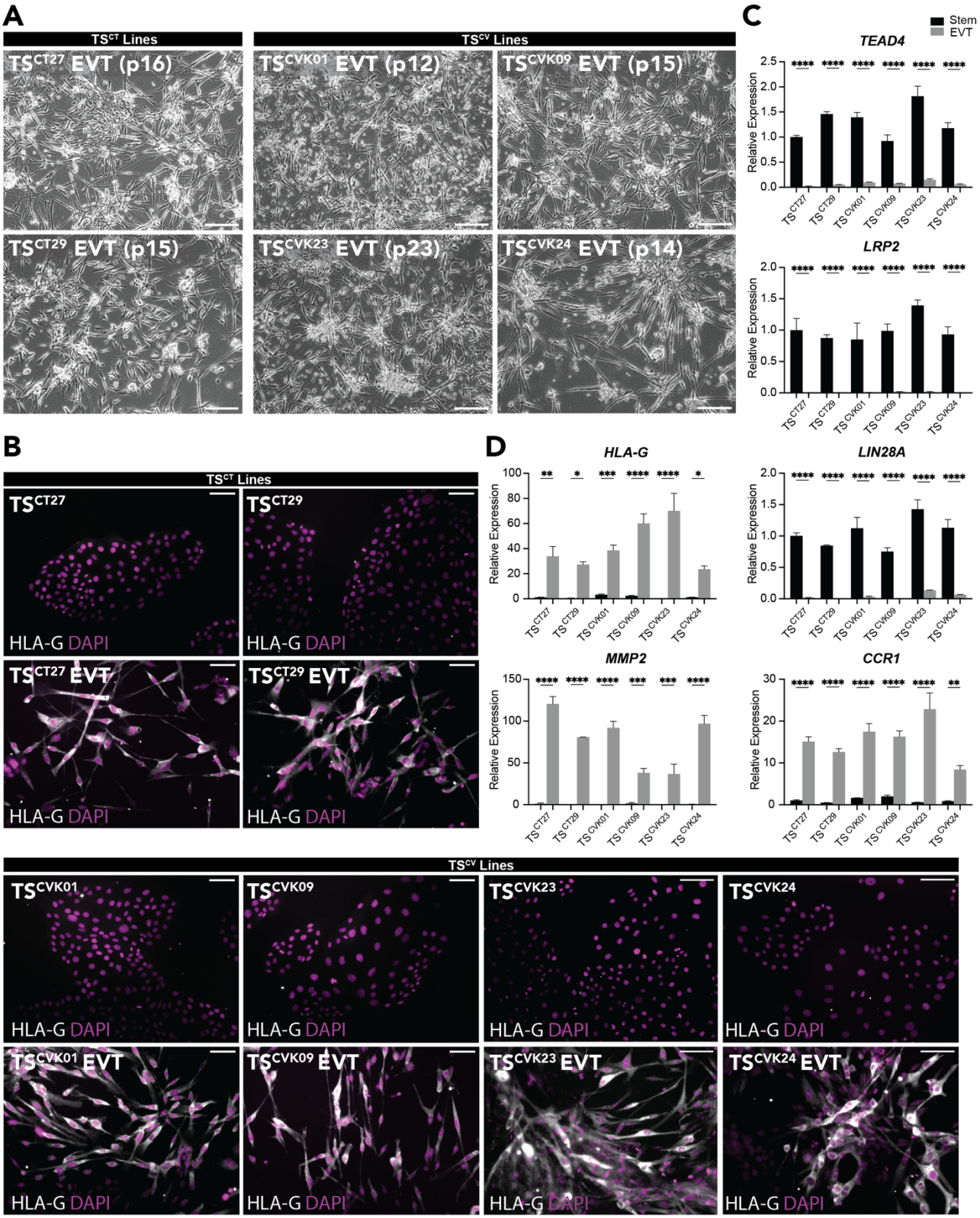

Fig. 4 TS^{CV} cell line differentiation into EVT cells. A) Representative phase contrast images of cytotrophoblast-derived TS^{CT27} and TS^{CT29} cells and four chorionic villus-derived TS cell lines possessing a normal karyotype, TS^{CVK01}, TS^{CVK09}, TS^{CVK23}, and TS^{CVK24} cells cultured under EVT

842 cell differentiation conditions. Scale bars represent 250 µm **B)** Immunofluorescence detection of
843 HLA-G (gray) by immunocytochemistry in TS^{CT} and TS^{CV} cells cultured in the stem state and on
844 day 8 of EVT cell differentiation. DAPI (magenta) stains cell nuclei. Scale bars represent 100
845 µm. **C-D)** Stem cell-associated transcripts (**C;** *TEAD4*, *LRP2*, and *LIN28A*) and EVT cell-
846 associated transcripts (**D**; *HLA-G*, *MMP2*, and *CCR1*) were quantified by RT-qPCR in stem
847 (black) and EVT differentiated (gray) TS^{CT27}, TS^{CT29}, TS^{CVK01}, TS^{CVK09}, TS^{CVK23}, and TS^{CVK24} cells
848 (n=3 samples per group; *p<0.05, **p<0.01, ***p<0.001, ****p<0.0001).

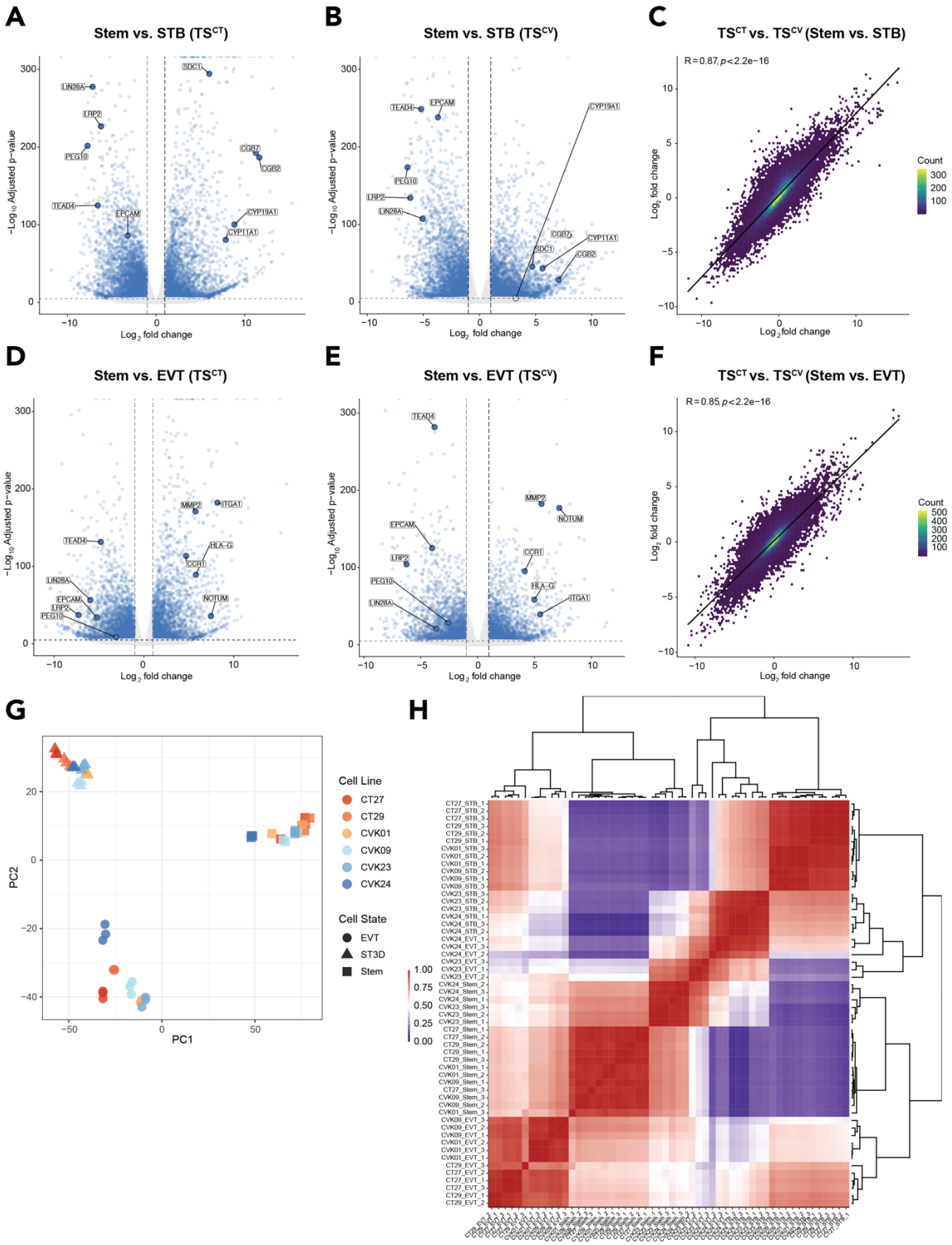
A
Stem vs. STB (TS^CT)
B
Stem vs. STB (TS^CV)
C
TS^CT vs. TS^CV (Stem vs. STB)
R=0.87, p<2.2e−16
Count
D
Stem vs. EVT (TS^CT)
E
Stem vs. EVT (TS^CV)
F
TS^CT vs. TS^CV (Stem vs. EVT)
R=0.85, p<2.2e−16
Count
−Log10 Adjusted p−value
Log2 fold change
G
PC1
PC2
Cell Line
CT27
CT29
CVK01
CVK09
CVK23
CVK24
Cell State
EVT
ST3D
Stem
H

849

850 **Fig. 5 TS^{CV} and TS^{CT} cells cluster by cell state and share similar transcriptomes. A-B)**
851 Volcano plots depicting significantly up- and down-regulated genes based on transcripts
852 measured by RNA-seq in stem versus STB state TS^{CT} (**A**) and TS^{CV} (**B**) cells. Gene transcript
853 levels unchanged between stem and STB state cells are depicted in gray (n=3 per group;
854 absolute Log_2 fold change >1, adjusted p<0.05). **C)** Two-dimensional density plot comparing
855 gene expression changes between stem and STB cell states in TS^{CT} (TS^{CT27} and TS^{CT29}) cells
856 versus TS^{CV} (TS^{CVK01}, TS^{CVK09}, TS^{CVK23}, and TS^{CVK24}) cells (Pearson correlation coefficient
857 (R)=0.87, p<2.2e-16). **D-E)** Volcano plots depicting significantly up- and down-regulated genes
858 based on transcripts measured by RNA-seq in stem versus EVT states of TS^{CT} (**E**) and TS^{CV} (**E**)
859 cells. Gene transcript levels unchanged between stem and EVT state cells are depicted in gray
860 (n=3 per group; absolute Log_2 fold change >1, adjusted p<0.05). **F)** Two-dimensional density
861 plot comparing gene expression changes between stem and EVT cell states in TS^{CT} (TS^{CT27} and
862 TS^{CT29}) cells versus TS^{CV} (TS^{CVK01}, TS^{CVK09}, TS^{CVK23}, and TS^{CVK24}) cells (Pearson correlation
863 coefficient (R)=0.85, p<2.2e-16). **G)** Principal component analysis based on RNA-seq datasets
864 generated from TS^{CT} and TS^{CV} cells cultured in the stem state or following differentiation into
865 STB and EVT cell lineages. **H)** Heat map showing scaled normalized read counts representing
866 gene expression profiles of stem state, STB, and EVT differentiated cells across TS^{CT} and TS^{CV}
867 cell lines.

868 **Video Legends**
869
870 **Video 1. Stem state and EVT-differentiated TS^{CT27} cell growth and motility.** Phase contrast
871 images were acquired every 10 min for 53 h of TS^{CT27} cells cultured under stem state or EVT
872 cell-differentiation conditions (EVT cell differentiation protocol days 4-6).
873
874 **Video 2. Stem state and EVT cell differentiated TS^{CVK01} cell growth and motility.** Phase
875 contrast images were acquired every 10 min for 53 h of TS^{CVK01} cells cultured under stem state
876 or EVT cell differentiation conditions (EVT cell differentiation protocol days 4-6).
877
878 **Video 3. Stem state and EVT cell differentiated TS^{CVK09} cell growth and motility.** Phase
879 contrast images were acquired every 10 min for 53 h of TS^{CVK09} cells cultured under stem state
880 or EVT cell differentiation conditions (EVT cell differentiation protocol days 4-6).